Generalized Non-Orthogonal Joint Diagonalization With LU Decomposition and Successive Rotations

Xiao-Feng Gong, *Member, IEEE*, Xiu-Lin Wang, and Qiu-Hua Lin, *Member, IEEE*

***Abstract*—Non-orthogonal joint diagonalization (NJD) free of prewhitening has been widely studied in the context of blind source separation (BSS) and array signal processing, etc. However, NJD is used to retrieve the jointly diagonalizable structure for a single set of target matrices which are mostly formulized with a single dataset, and thus is insufficient to handle multiple datasets with inter-set dependences, a scenario often encountered in joint BSS (J-BSS) applications. As such, we present a generalized NJD (GNJD) algorithm to simultaneously perform asymmetric NJD upon multiple sets of target matrices with mutually linked loading matrices, by using LU decomposition and successive rotations, to enable J-BSS over multiple datasets with indication/exploitation of their mutual dependences. Experiments with synthetic and real-world datasets are provided to illustrate the performance of the proposed algorithm.**

***Index Terms*—Blind source separation, joint diagonalization, LU decomposition, successive rotation.**

I. Introduction

JOINT DIAGONALIZATION (JD) is an important instrument in solving blind source separation (BSS) problems. For example, consider an instantaneous linear mixture $\boldsymbol{x}(t) = \boldsymbol{A}\boldsymbol{s}(t) \in \mathbb{C}^N$, where $\boldsymbol{s}(t) \in \mathbb{C}^N$ and $\boldsymbol{A} \in \mathbb{C}^{N\times N}$ denote the source and mixing matrix, respectively. The sources are assumed mutually independent, or uncorrelated but with some temporal structures (e.g., non-stationarity, non-whiteness). We can then calculate the 4th-order cumulant [1] or 2nd-order covariance matrices (at distinct time instants or time shifts) [2]–[4] $\boldsymbol{C}_1, \ldots, \boldsymbol{C}_K$ under the above assumptions, that share the following jointly diagonalizable structure:

$$\boldsymbol{C}_k = \boldsymbol{A}\boldsymbol{D}_k\boldsymbol{A}^H \tag{1}$$

where $\boldsymbol{D}_k$ is diagonal, $k = 1, \ldots, K$, and superscript 'H' denotes conjugated transpose. JD then seeks an estimate of $\boldsymbol{A}$ by fitting the above common JD structure.

Numerous algorithms for computing JD were proposed in the open literature. While the early works are mostly focused on orthogonal JD (OJD) which requires $\boldsymbol{A}$ to be unitary and thus applied in BSS of pre-whitened mixtures [1], [2], the recent efforts, on the other hand, turned to non-orthogonal JD (NJD) to facilitate BSS free of pre-whitening for both real-valued and complex-valued mixtures [3]–[14]. Criteria including weighted least squares [4]–[8], minimization of off-norm [9]–[13], and information theoretic criterion [14] were successfully adopted, that are specifically accomplished via several optimization strategies such as Gauss-Newton [8] and successive rotations [10]–[14].

Although JD has found growing interests in both theory and application, the majority of its contributions are with regards to single-set data analysis such as BSS of a single set of linear instantaneous mixtures. More precisely, the target matrices for JD are mostly formulized by computing the intra-set statistics (e.g., auto-covariance, 4th-order cumulant) of a single dataset, and are thus with symmetric or Hermitian structure. In this background, most of the JD works were historically devised for symmetric or Hermitian target matrices whose row and column spaces are identical [1]–[14]. However, when multiple datasets with inter-set dependences are available, for example, when working on multi-subject/multi-modal biomedical data fusion problems [15], [20]–[23], or BSS of transformed signals in multiple frequency bins [16], the use of NJD fails to sufficiently utilize these inter-set dependences, and this will explicitly result in problems such as permutation misalignment or loss of accuracy [24], [25]. As such, generalized JD (GJD), that incorporates both intra-set and inter-set statistics to enable joint BSS (J-BSS) of multi-set data, has become an issue of great interests. Indeed, although J-BSS has already been addressed in other aspects of BSS, for example, in independent vector analysis (IVA) [15]–[17], canonical correlation analysis (CCA) [18], [19], [22], and multi-set CCA (MCCA) [20]–[22], efforts with GJD towards J-BSS are still limited [24]–[29]. The main difficulty lies in the fact that calculating inter-set statistics brings asymmetric target matrices for GJD, yet the derivations for most of the existing JD works were devised for symmetric or Hermitian problems.

More precisely, asymmetric OJD or joint SVD (J-SVD) was studied in [25], which could be used for J-BSS of 2 pre-whitened datasets. The work in [24], [26] considered generalized OJD (GOJD) problem, to facilitate J-BSS of 3 or more pre-whitened datasets. The authors of [26] also considered for the first time non-orthogonal joint BSS (NOJoB) for 3 or more datasets within the generalized NJD (GNJD) context. This algorithm was originally devised for real-valued problems, and could be extended to the complex case with some tiny

Manuscript received August 28, 2014; revised December 28, 2014; accepted December 30, 2014. Date of publication January 12, 2015; date of current version February 04, 2015. The associate editor coordinating the review of this manuscript and approving it for publication was Prof. Adel Belouchrani. This work was supported in part by Doctoral Fund of Ministry of Education of China under grant 20110041120019, National Natural Science Foundation of China under grants 61072098, 61105008, 61331019, 61379012, and Scientific Research Fund of Liaoning Provincial Education Department under grant L2014016.

The authors are with the School of Information and Communication Engineering, Dalian University of Technology, Dalian, China, 116024 (e-mail: xfgong@dlut.edu.cn; wxl1482@mail.dlut.edu.cn; qhlin@dlut.edu.cn).

Color versions of one or more of the figures in this paper are available online at http://ieeexplore.ieee.org.

Digital Object Identifier 10.1109/TSP.2015.2391074

modifications. We also considered in [27] the joint solution of multiple asymmetric NJD problems as a preliminary work of the presented one. However, the joint NJD (JNJD) algorithm therein makes use of dependences between adjacent datasets only, and thus still has problems when handling large number of datasets. In addition, several GJD algorithms have been successfully applied to constrained or coupled tensor factorization problems [28], [29]. More precisely, the canonical polyadic decomposition (CPD) with constraints of constant modulus was converted into a simple GJD formulation in [28], such that 2 sets of target matrices (one set is Hermitian and the other is symmetric) with a common loading matrix are handled simultaneously. In [29], we considered coupled CPD of 2 tensors with a shared loading matrix and demonstrated how it could be solved with the JNJD algorithm developed in [27].

In this study, we propose another GNJD algorithm for the joint analysis of multiple datasets. More specifically, the GNJD problem is set up with multiple asymmetric NJD problems, of which every two distinct ones are linked by a shared loading matrix. By exploiting these mutual links across datasets, the multiple asymmetric NJD problems are solved simultaneously using LU decomposition and successive elementary rotations. The proposed GNJD algorithm relieves the orthogonality constraints for J-SVD and GOJD, and could be used to handle 3 or more datasets. In addition, when compared with NOJoB, we note that similar problem is considered but with distinct optimization strategies. In particular, the proposed GNJD algorithm yields better convergence behavior when handling large number of datasets, and improved performance in high noise levels, as will be shown later.

The rest of the paper is organized as follows. In Section II, we give the formulization of the GNJD problem and some examples on how practical problems could be linked to GNJD. In Section III, we present the proposed algorithm as well as theoretical analysis including computational complexity and convergence, and some implementation remarks. Experiment results are given in Section IV to illustrate the performance of the proposed algorithm. Finally, Section V concludes this paper. The source programs for the proposed algorithm are available at [39].

II. Problem Formulation

In this section, we present the data model for multi-set processing and further give examples on how the multi-set data model could be formulized into GNJD problems. In addition, comparisons with existing JD and GJD formulizations are also given to provide insights into the GNJD model.

A. Multi-Set Data Model

Recently, multi-set data processing has attracted much attention in the literature [15]–[27]. The key idea to these works is to incorporate both intra-set independence (as is assumed in classical BSS problems) and inter-set dependence at the source level, to achieve J-BSS or data fusion for multiple datasets. The following multi-set instantaneous mixing model is assumed:

$$\boldsymbol{x}_r(t) = \boldsymbol{A}_r \boldsymbol{s}^{(r)}(t), \quad r = 1, 2, \ldots, R \tag{2}$$

where $\boldsymbol{x}_r(t), \boldsymbol{s}^{(r)}(t) \in \mathrm{C}^N, \boldsymbol{A}_r \in \mathrm{C}^{N \times N}$ denote the observation, source, and mixing matrix in the rth dataset, respectively, $r = 1, 2, \ldots, R$. By defining new source vectors:

$$\boldsymbol{s}_n(t) \triangleq \left[s_n^{(1)}(t), \ldots, s_n^{(R)}(t)\right]^T \in \mathrm{C}^R, \quad n = 1, \ldots, N \tag{3}$$

we note that $\boldsymbol{s}_n(t)$ and $\boldsymbol{s}_m(t)$ are independent for any $1 \leq m \neq n \leq N$ (intra-set independence), and that components of $\boldsymbol{s}_n(t)$ are mutually dependent (inter-set dependence).

The above multi-set data model has been largely considered in practical problems. For example, in BSS of convolutive mixtures, (2) models the linear mixing procedure at the rth frequency bin, and the inter-set dependence mentioned above formulizes the well-known cross frequency dependences that are extensively used in frequency domain BSS of convolutive mixtures [16].

The above model is also widely used in multi-set data fusion with emphasis on finding their similarities or connections, and has found applications in biomedical engineering [15], [20]–[23]. For example, the multiple datasets might refer to data of different modalities (e.g., fMRI, EEG, sMRI) collected from a single subject under equal conditions, and joint analysis methods that simultaneously decompose these datasets with indications of their relations are of high interests [21], [22]. Moreover, the multiple datasets could as well refer to those collected from multiple subjects under identical modality and conditions. Typical examples include multi-subject fMRI data and hyper-scanning EEG data [20], [23]. In addition, the above multi-set data model was also used in array processing applications to formulate signals collected from distinct sensors (e.g., electrocardiogram data collected with multi-electrodes [24]), or array statistics of distinct orders or forms (e.g., covariance and pseudo-covariance matrices [29]).

B. GNJD Formulation

The GNJD formulation contains $(R+1)R/2$ sets of NJD problems (mostly asymmetric) of the following form:

$$\boldsymbol{C}_{r_1,r_2,k} \triangleq \boldsymbol{A}_{r_1} \cdot \boldsymbol{D}_{r_1,r_2,k} \cdot \boldsymbol{A}_{r_2}^H \tag{4}$$

where $\boldsymbol{A}_{r_1}, \boldsymbol{A}_{r_2} \in \mathrm{C}^{N \times N}$ denote loading matrices for the r_1th and r_2th datasets, $\boldsymbol{C}_{r_1,r_2,k}, \boldsymbol{D}_{r_1,r_2,k} \in \mathrm{C}^{N \times N}$, denote the target matrices and the unloaded diagonal matrices, respectively, $k = 1, \ldots, K$, $1 < r_1 \leq r_2 < R$. Integers R, K and N denote the number of loading matrices, number of target matrices in each NJD dataset, and dimensionality of target matrices, respectively. We note that the (r_1, r_2)th set of target matrices share with the (r_1, l)th and (l', r_2)th sets the loading matrices $\boldsymbol{A}_{r_1}$ and $\boldsymbol{A}_{r_2}$, respectively, $l = r_1, \ldots, R$, $l' = 1, \ldots, r_2$. Therefore, all these $(R+1)R/2$ NJD problems are mutually connected with one another. GNJD then aims at estimating all the R loading matrices $\boldsymbol{A}_1, \boldsymbol{A}_2, \ldots, \boldsymbol{A}_R$ such that the jointly diagonalizable structures for all the $(R+1)R/2$ NJD problems in (4) are fitted simultaneously.

It is important to note that the above GNJD formulation could be derived from the multi-set data model provided in

Subsection II.A. For example, with source non-stationarity present we could calculate the following target matrices:

$$\begin{aligned}\boldsymbol{C}_{r_1,r_2,k} &\triangleq \mathrm{E}\left\{\boldsymbol{x}_{r_1}(k)\left[\boldsymbol{x}_{r_2}(k)\right]^H\right\} \\ &= \boldsymbol{A}_{r_1}\mathrm{E}\left\{\boldsymbol{s}^{(r_1)}(k)\left[\boldsymbol{s}^{(r_2)}(k)\right]^H\right\}\boldsymbol{A}_{r_2}^H \end{aligned} \tag{5}$$

where $r_1, r_2 = 1, 2, \ldots, R$. Moreover, we note here that $E\{\boldsymbol{s}^{(r_1)}(k) \cdot [\boldsymbol{s}^{(r_2)}(k)]^H\}$ is diagonal under the basic assumptions of J-BSS of intra-set independence and inter-set dependence, and thus (5) is actually a GNJD formulation. In addition, the GNJD formulization could also be obtained by calculating the cross 4th-order cumulants upon the multi-set data model, as is done in [24].

C. Comparison With Existing Formulations for BSS and J-BSS

The considered GNJD model is distinct from the NJD models as well as some other linear algebraic models that are well-established for BSS and J-BSS. More exactly, we note that the majority of NJD works considered symmetric or Hermitian target matrices [1]–[14], which were usually constructed with 2nd-order or 4th-order intra-set statistics (such as covariance) of single dataset observations[1]. Therefore, the NJD works are mostly devoted to BSS of a single dataset, and the reasonings therein might be invalid for asymmetric NJD problems (in the sense that the row and column spaces are distinct) involved in the GNJD formulation.

For the joint analysis of 2 datasets, some linear algebraic models have been established by calculating inter-set statistics across the 2 datasets. The classical CCA method is one such example, for which the cross-covariance matrix of 2 datasets is established as the sole target matrix [18], [19], and [22]. The work in [25] further extends the above one sample cross-covariance model in CCA into multiple samples to form an asymmetric JD (or J-SVD) model. It is important to note that the above CCA and asymmetric JD models could be considered as special cases of GNJD. More exactly, GNJD model in (4) degrades to the asymmetric JD model if we let $R = 2$, $r_1 = 1$ and $r_2 = 2$, which is further reduced to CCA if we set K to 1.

Recently, some advanced models were developed for multiple datasets (more than 2). In particular, the MCCA model extends CCA so as to include one sample cross-covariance matrices among every 2 pre-whitened datasets [20]–[22]. The GOJD model considered in [24] further extends MCCA to the multi-sample case. In particular, GNJD model could be converted into GOJD if we require the loading matrices $\boldsymbol{A}_r$'s to be unitary, $r = 1, 2, \ldots, R$, and that r_2 be strictly larger than r_1, and GOJD could be further converted into MCCA if we set K to 1. In addition, GNJD is also different from the JNJD formulation in [27], if we note that JNJD only considered a subset of GNJD model with $r_2 = r_1 + 1$.

As a result, GNJD is a more generalized model for multi-set data analysis than the existing CCA, asymmetric JD, MCCA, GOJD, and JNJD models. In addition, we note that the above models for multi-set analysis are distinct from ordinary NJD in that the latter fails to consider the inter-set dependences. In particular, advantages of using multi-set models over NJD have been partially addressed in [25], [27], with respects to permutation alignment and estimation accuracy.

To our best knowledge, the above GNJD model has only been considered once in the open literature [26], where a non-orthogonal joint BSS (NOJoB) algorithm was proposed based on power iterations. However, this algorithm will occasionally suffer from non-optimal converging patterns and performance loss in highly noisy environment, as will be shown in the experiment section. In the next section, we propose an algorithm to solve the GNJD problem with LU decomposition and successive rotations.

III. Proposed Algorithm

In this section, we illustrate how the GNJD problem is solved with LU decomposition and successive elementary rotations. In addition, we present some analysis and implementation remarks to provide insights into the proposed algorithm.

A. GNJD With LU Decomposition and Successive Rotations

To solve the GNJD problem, we extend the well-established off-norm minimization criterion [9]–[13] to GNJD as follows:

$$\begin{aligned}&\{\boldsymbol{B}_1, \ldots, \boldsymbol{B}_R\} \\ &\quad = \underset{\boldsymbol{B}_1,\ldots,\boldsymbol{B}_R}{\arg\min} \sum_{k=1}^{K}\sum_{r_2=r_1}^{R}\sum_{r_1=1}^{R}\left\|\mathrm{off}\left(\boldsymbol{B}_{r_1}\cdot\boldsymbol{C}_{r_1,r_2,k}\cdot\boldsymbol{B}_{r_2}^H\right)\right\|_F^2 \end{aligned} \tag{6}$$

where $\boldsymbol{B}_r \triangleq \boldsymbol{A}_r^{-1}$ denotes the rth unloading matrix, $\mathrm{off}(\,\cdot\,)$ is the operator that sets all the diagonal elements of its entry to zero, and $\|\cdot\|_F$ is Frobenius norm.

We note that the problem in (6) involves lots of parameters to adjust during the optimization. Therefore, we adopt LU decomposition and successive rotation based scheme to ease this problem into loops over simple linear sub-optimizations [1], [10]–[14], [27]. More exactly, we consider the LU decomposition of $\boldsymbol{B}_r$, $r = 1, 2, \ldots, R$:

$$\boldsymbol{B}_r = \boldsymbol{L}_r\boldsymbol{U}_r \tag{7}$$

where $\boldsymbol{L}_r, \boldsymbol{U}_r \in \mathrm{C}^{N\times N}$ are the rth lower-triangular and upper-triangular matrices, respectively, $r = 1, \ldots, R$, and then (6) could be converted into the following 2 alternating stages, which update either $\boldsymbol{L}_r$ or $\boldsymbol{U}_r$ one at a time:

$$\begin{aligned}&\{\tilde{\boldsymbol{U}}_r | r = 1, \ldots, R\} \\ &\quad = \underset{\tilde{\boldsymbol{U}}_1,\ldots,\tilde{\boldsymbol{U}}_R}{\arg\min} \sum_{k=1}^{K}\sum_{r_2=r_1}^{R}\sum_{r_1=1}^{R}\left\|\mathrm{off}\left(\tilde{\boldsymbol{U}}_{r_1}\boldsymbol{C}_{r_1,r_2,k}\tilde{\boldsymbol{U}}_{r_2}^H\right)\right\|_F^2 \end{aligned} \tag{8}$$

$$\begin{aligned}&\{\tilde{\boldsymbol{L}}_r | r = 1, \ldots, R\} \\ &\quad = \underset{\tilde{\boldsymbol{L}}_1,\ldots,\tilde{\boldsymbol{L}}_R}{\arg\min} \sum_{k=1}^{K}\sum_{r_2=r_1}^{R}\sum_{r_1=1}^{R}\left\|\mathrm{off}\left(\tilde{\boldsymbol{L}}_{r_1}\boldsymbol{C'}_{r_1,r_2,k}\tilde{\boldsymbol{L}}_{r_2}^H\right)\right\|_F^2 \end{aligned} \tag{9}$$

where $\boldsymbol{C'}_{r_1,r_2,k} = \tilde{\boldsymbol{U}}_{r_1}\boldsymbol{C}_{r_1,r_2,k}\tilde{\boldsymbol{U}}_{r_2}^H$, $\tilde{\boldsymbol{U}}_r, \tilde{\boldsymbol{L}}_r$ denote the updates of $\boldsymbol{U}_r, \boldsymbol{L}_r$. In the proposed algorithm, (8) and (9) are alternated

[1] Sometimes the target matrices may neither be symmetric nor Hermitian such as the complex time-lagged covariance matrices [2]. We note that the row and column spaces of these target matrices are identical, and thus the target matrices could be converted into Hermitian by adding with their conjugated transposes.

until convergence is reached. Next we shall explain how these 2 sub-optimization problems could be solved using successive rotations. Before we start, we note that these 2 stages are similar as they both seek estimates for triangular matrices, and thus we shall only discuss the L-stage in (9).

More exactly, the updating of $\{\tilde{\boldsymbol{L}}_r|r=1,\ldots,R\}$ is in terms of successive products of elementary rotation matrices, each associated with an index pair (i,j), by repeatedly solving the following sub-optimization problems for all index pairs (i,j) [see (10) at the bottom of the page]: where $\boldsymbol{T}_{r,(i,j)}$ is the elementary rotation matrix associated with index pair (i,j). $\boldsymbol{C}_{r_1,r_2,k,\text{new}}$, $\boldsymbol{L}_{r,\text{new}}$ are the most recent updates for $\boldsymbol{C}_{r_1,r_2,k}$ and $\boldsymbol{L}_r$, and $\boldsymbol{C}_{r_1,r_2,k,\text{old}}$, $\boldsymbol{L}_{r,\text{old}}$ are updates in the previous iteration. We note that $\boldsymbol{T}_{r,(i,j)}$ is an elementary lower triangular matrix defined as:

$$\boldsymbol{T}_{r,(i,j)} \triangleq \begin{bmatrix} 1 & & & & \\ & \ddots & & & \\ & & 1 & & \\ & \alpha_{r,(i,j)} & & \ddots & \\ & & & & 1 \end{bmatrix} \tag{11}$$

where the only non-zero off-diagonal element $\alpha_{r,(i,j)}$ is at the ith row and jth column. As such, we only need to estimate 2 sets of parameters $\{\alpha_{r_1,(i,j)}|r_1=1,\ldots,R\}$ and $\{\alpha_{r_2,(i,j)}|r_2=r_1,\ldots,R\}$ by minimizing $\zeta_{(i,j),\text{new}} = \sum_{k=1}^{K}\sum_{r_2=r_1}^{R}\sum_{r_1=1}^{R}\|\text{off}(\boldsymbol{T}_{r_1,(i,j)}\boldsymbol{C}_{r_1,r_2,k,\text{old}}\boldsymbol{T}_{r_2,(i,j)}^{H})\|_F^2$ in each iteration, formulized as:

$$\begin{aligned}\zeta_{(i,j),\text{new}} &= \sum_{r_2=r_1}^{R}\sum_{r_1=1}^{R}\sum_{k=1}^{K}\sum_{p=1,p\neq i}^{N}\Big(|\boldsymbol{C}_{r_1,r_2,k,\text{new}}(i,p)|^2 \\ &\quad + |\boldsymbol{C}_{r_1,r_2,k,\text{new}}(p,i)|^2\Big) \\ &= \sum_{r=1}^{R}\sum_{k=1}^{K}\sum_{p=1,p\neq i}^{N}\left(\sum_{r_2=r}^{R}|\boldsymbol{C}_{r,r_2,k,\text{new}}(i,p)|^2\right. \\ &\quad \left. + \sum_{r_1=1}^{r}|\boldsymbol{C}_{r_1,r,k,\text{new}}(p,i)|^2\right)\end{aligned} \tag{12}$$

by denoting $\boldsymbol{C}_{r_1,r_2,k,\text{new}} = \boldsymbol{T}_{r_1,(i,j)}\boldsymbol{C}_{r_1,r_2,k,\text{old}}\boldsymbol{T}_{r_2,(i,j)}^{H}$ and noting that multiplying $\boldsymbol{C}_{r_1,r_2,k,\text{old}}$ from the left and right with $\boldsymbol{T}_{r_1,(i,j)}$ and $\boldsymbol{T}_{r_2,(i,j)}^{H}$ only impact its ith row and column, respectively.

Moreover, with some simple operations we could express $|\boldsymbol{C}_{r_1,r_2,k,\text{new}}(i,p)|^2$ and $|\boldsymbol{C}_{r_1,r_2,k,\text{new}}(p,i)|^2$ explicitly with $\alpha_{r_1,(i,j)}$ and $\alpha_{r_2,(i,j)}$ as follows:

$$\begin{aligned}&|\boldsymbol{C}_{r_1,r_2,k,\text{new}}(i,p)|^2 \\ &= \Big[|\boldsymbol{C}_{r_1,r_2,k,\text{old}}(j,p)|^2\,\alpha_{r_1,(i,j)}\alpha_{r_1,(i,j)}^{*} \\ &\quad + \boldsymbol{C}_{r_1,r_2,k,\text{old}}(i,p)\boldsymbol{C}_{r_1,r_2,k,\text{old}}^{*}(j,p)\alpha_{r_1,(i,j)}^{*} \\ &\quad + \boldsymbol{C}_{r_1,r_2,k,\text{old}}(j,p)\boldsymbol{C}_{r_1,r_2,k,\text{old}}^{*}(i,p)\alpha_{r_1,(i,j)} \\ &\quad + |\boldsymbol{C}_{r_1,r_2,k,\text{old}}(i,p)|^2\Big]\end{aligned} \tag{13}$$

$$\begin{aligned}&|\boldsymbol{C}_{r_1,r_2,k,\text{new}}(p,i)|^2 \\ &= \Big[|\boldsymbol{C}_{r_1,r_2,k,\text{old}}(p,j)|^2\,\alpha_{r_2,(i,j)}\alpha_{r_2,(i,j)}^{*} \\ &\quad + \boldsymbol{C}_{r_1,r_2,k,\text{old}}(p,j)\boldsymbol{C}_{r_1,r_2,k,\text{old}}^{*}(p,i)\alpha_{r_2,(i,j)}^{*} \\ &\quad + \boldsymbol{C}_{r_1,r_2,k,\text{old}}(p,i)\boldsymbol{C}_{r_1,r_2,k,\text{old}}^{*}(p,j)\alpha_{r_2,(i,j)} \\ &\quad + |\boldsymbol{C}_{r_1,r_2,k,\text{old}}(p,i)|^2\Big]\end{aligned} \tag{14}$$

Substituting (13) and (14) into (12) yields:

$$\begin{aligned}&\zeta_{(i,j),\text{new}} \\ &= \sum_{r=1}^{R}\sum_{k=1}^{K}\sum_{p=1,p\neq i}^{N}\Big[a_{j,p,r}|\alpha_{r,(i,j)}|^2 + b_{i,j,p,r}\alpha_{r,(i,j)}^{*} \\ &\quad + b_{i,j,p,r}^{*}\alpha_{r,(i,j)} + a_{i,p,r}\Big]\end{aligned} \tag{15}$$

where $a_{j,p,r}$, $b_{i,j,p,r}$ are defined as (16), shown at the bottom of the page.

By defining $\zeta_{(i,j),r} \triangleq \sum_{k=1}^{K}\sum_{p=1,p\neq i}^{N} a_{j,p,r}|\alpha_{r,(i,j)}|^2 + b_{i,j,p,r}\alpha_{r,(i,j)}^{*} + b_{i,j,p,r}^{*}\alpha_{r,(i,j)} + a_{i,p,r}$, we actually express $\zeta_{(i,j),\text{new}}$ as summation of R terms: $\zeta_{(i,j),\text{new}} = \sum_{r=1}^{R}\zeta_{(i,j),r}$, and each term $\zeta_{(i,j),r}$ is associated with only one parameter $\alpha_{r,(i,j)}$, $r=1,\ldots,R$. Therefore, we need only set the derivative of $\zeta_{(i,j),r}$ with respect to $\alpha_{r,(i,j)}^{*}$ to zero, for the estimation of $\alpha_{r,(i,j)}$. The solution is given below:

$$\tilde{\alpha}_{r,(i,j)} = -\left(\sum_{k=1}^{K}\sum_{p=1,p\neq i}^{N} a_{j,p,r}\right)^{-1}\left(\sum_{k=1}^{K}\sum_{p=1,p\neq i}^{N} b_{i,j,p,r}\right) \tag{17}$$

The L-stage constitutes sweeps over all the index pairs (i,j), $1 \le j < i \le N$, as is given in (10), with the optimal parameters found with (17). When all the possible index pairs are exhausted once (one sweep), we switch to the U-stage that is accomplished

$$\begin{cases}\{\boldsymbol{T}_{r,(i,j)}|r=1,\ldots,R\} = \underset{\boldsymbol{T}_1,\ldots,\boldsymbol{T}_R}{\arg\min}\displaystyle\sum_{k=1}^{K}\sum_{r_2=r_1}^{R}\sum_{r_1=1}^{R}\left\|\text{off}\left(\boldsymbol{T}_{r_1,(i,j)}\boldsymbol{C}_{r_1,r_2,k,\text{old}}\boldsymbol{T}_{r_2,(i,j)}^{H}\right)\right\|_F^2 \\ \boldsymbol{C}_{r_1,r_2,k,\text{new}} = \boldsymbol{T}_{r_1,(i,j)}\boldsymbol{C}_{r_1,r_2,k,\text{old}}\boldsymbol{T}_{r_2,(i,j)}^{H}, \qquad \boldsymbol{L}_{r,\text{new}} = \boldsymbol{T}_{r,(i,j)}\boldsymbol{L}_{r,\text{old}}\end{cases} \tag{10}$$

$$\begin{cases} a_{j,p,r} \triangleq \sum_{r_2=r}^{R}|\boldsymbol{C}_{r,r_2,k,\text{old}}(j,p)|^2 + \sum_{r_1=1}^{r}|\boldsymbol{C}_{r_1,r,k,\text{old}}(p,j)|^2 \\ b_{i,j,p,r} \triangleq \sum_{r_2=r}^{R}\boldsymbol{C}_{r,r_2,k,\text{old}}(i,p)\boldsymbol{C}_{r,r_2,k,\text{old}}^{*}(j,p) + \sum_{r_1=1}^{r}\boldsymbol{C}_{r_1,r,k,\text{old}}(p,j)\boldsymbol{C}_{r_1,r,k,\text{old}}^{*}(p,i)\end{cases} \tag{16}$$

similarly to the L-stage, with the only exception that the index pair satisfy $1 \leq i < j \leq N$. Then after one sweep for the U-stage we return to the L-stage. These 2 stages are alternated one after another until convergence.

B. Remarks and Discussion

In this subsection we provide discussions on the properties of the proposed GNJD algorithm, such as computation complexity and convergence, as well as some implementation remarks.

Remark 1 (Computation Complexity Per Sweep): From (10) and (17) we note that in each iteration for fixed index pair (i,j) in L-stage, the load for calculating $\tilde{\alpha}_{r,(i,j)}$, $r = 1, \ldots, R$ is $\mathcal{O}(2NKR^2)$, and those for updating $\boldsymbol{C}_{r_1,r_2,k}$ and $\boldsymbol{L}_{r,k}$ are $\mathcal{O}(NKR^2)$ and NR, respectively. Therefore, taking into consideration that there exist $N(N-1)/2$ such iterations in each sweep and that similar analysis holds for U-stage as well, the overall computation load per sweep of GNJD is $\mathcal{O}(3KR^2N^3)$. In addition, with similar analysis we note that the computation complexities for JNJD, NOJoB, and GOJD are $\mathcal{O}(6KRN^3)$, $\mathcal{O}(2KR^2N^3)$and $\mathcal{O}(3KR^2N^3)$, respectively. We note here that the computation load per sweep of GNJD is comparable to that of GOJD, while JNJD is the least complex as it uses much less target matrices in the computation procedure.

Remark 2 (Convergence): It is important to note that the transformation in (10) always reduces the cost function defined in (6) for each iteration. More exactly, if we take the L-stage for example, the cost function in the iteration with index pair (i,j) is reduced to (15) since only the ith columns and rows of the target matrices are updated. Therefore, substituting the solution $\tilde{\alpha}_{r,(i,j)}$ into (15), we have the following result:

$$\begin{aligned} \Delta\zeta &\triangleq \zeta_{(i,j),\text{new}} - \zeta_{(i,j),\text{old}} \\ &= -\frac{\sum\limits_{r=1}^{R}\sum\limits_{k=1}^{K}\sum\limits_{p=1,p\neq i}^{N} |b_{i,j,p,r}|^2}{\sum\limits_{k=1}^{K}\sum\limits_{p=1,p\neq i}^{N} a_{j,p,r}} \end{aligned} \tag{18}$$

where $a_{j,p,r}$, $b_{i,j,p,r}$ are defined in (16). We note that $\Delta\zeta$ is always non-positive. Since the cost function is lower-bounded by zero by definition, and is always reduced by the proposed iterations as is implied by (18), the proposed algorithm is guaranteed to at least converge to a local minimum.

Remark 3 (Parallelization for Calculation of $\alpha_{r,(i,j)}$): We note that (17) actually infers parallel calculation of $\alpha_{r,(i,j)}$ for all $r = 1, \ldots, R$, instead of the dataset-wise sequential scheme that calculates $\alpha_{1,(i,j)}, \alpha_{2,(i,j)}, \ldots, \alpha_{R,(i,j)}$ one after another. Noting that the above sequential updating of unmixing matrix is required for NOJoB, the proposed GNJD algorithm is expected to perform faster than NOJoB when handling large number of datasets.

In addition, parallelization over matrix dimensionality could be considered for further acceleration [30], [31]. More exactly, we can use the column-wise parallelization scheme [30] that calculates all $\alpha_{r,(i,j)}$'s with identical i index yet distinct j indices simultaneously. It is interesting to note that this scheme is able to largely reduce the number of rotations needed in one particular sweep without losing any accuracy of calculation in the NJD context, and thus similar property could be expected for GNJD. Other parallelization schemes, such as the tournament player ordering scheme [31], could also be used in our GNJD method.

Remark 4 (On the Balance of Intra-Set Statistics and Inter-Set Statistics): We note that the cost function for GNJD could be rewritten as the sum of two terms as follows:

$$\begin{aligned} \eta = &\overbrace{\sum_{k=1}^{K}\sum_{r=1}^{R}\left\|\text{off}\left(\boldsymbol{B}_r \cdot \boldsymbol{C}_{r,r,k} \cdot \boldsymbol{B}_r^H\right)\right\|_F^2}^{\eta_1} \\ &+\overbrace{\sum_{k=1}^{K}\sum_{r_2=r_1+1}^{R}\sum_{r_1=1}^{R-1}\left\|\text{off}\left(\boldsymbol{B}_{r_1} \cdot \boldsymbol{C}_{r_1,r_2,k} \cdot \boldsymbol{B}_{r_2}^H\right)\right\|_F^2}^{\eta_2} \end{aligned} \tag{19}$$

In J-BSS applications, η_1 involves off-norms of target matrices $\boldsymbol{C}_{r,r,k}$'s that are calculated with intra-set statistics, such as auto-covariance within the rth dataset, yet η_2 is related to matrices $\boldsymbol{C}_{r_1,r_2,k}$, $r_1 < r_2$ that are usually obtained from inter-set statistics across datasets, such as cross-covariance or cross 4th-order cumulant matrices. Details on the calculation of these target matrices for J-BSS could be found in Subsection II.B. The goal of J-BSS is to: (1) estimate R unmixing matrices $\boldsymbol{B}_r$'s simultaneously, and (2) at the same time align the permutations of columns for all $\boldsymbol{B}_r$'s, $r = 1, 2, \ldots, R$ by minimizing η. It is important to note, with regards to the 2 terms η_1 and η_2, that minimizing η_1 only yields estimates of unmixing matrices without permutation alignment, yet minimization of η_2 achieves the same goal as J-BSS: estimation of unmixing matrices as well as permutation alignment. As such, the inter-set statistical target matrices actually play a more important role than the intra-set ones in achieving J-BSS, and this infers that we should give η_2 a larger portion in η when performing GNJD.

In addition, the numbers of intra-set statistical and inter-set statistical target matrices in GNJD model (4) are RK and $R(R-1)K/2$, respectively, and thus the portion of η_2 in η is roughly $(R-1)/(R+1)$, which is small when R takes small values. This indicates that using the cost function (19) might encounter some problem for small numbers of datasets with regards to permutation alignment. Indeed, a smaller portion of η_2 will result in a number of local minima in the manifold of the cost function that come from the intra-set statistics, and GNJD is likely to be stuck into a local minimum in such cases.

Indeed, we have observed with simulations quite a few non-optimal convergence patterns for NOJoB and GNJD when R takes small values, which in return verifies our analysis above. It is important to note that GOJD does not have such problem as it uses inter-set statistics only.

To solve the above problem, we consider to remove intra-set statistical target matrices from GNJD when R is smaller than R' (empirically set to 5), and remain both intra-set statistics and inter-set statistics otherwise.

Remark 5 (Termination Criteria): Several stopping criteria are available such as monitoring the changes of the off-norm based cost function defined in (6) between 2 adjacent sweeps. Here we choose to terminate the iterations when the overall updates of $\boldsymbol{L}_r$ and $\boldsymbol{U}_r$ from all the elementary matrices $\boldsymbol{T}_{r,(i,j)}$ are

TABLE I
IMPLEMENTATION OF PROPOSED ALGORITHM

```
● Input: $R(R+1)/2$ sets of target matrices $C_{r_1,r_2,k}$, $r_1 = 1,...,R$, $r_2 = r_1,...,R$, $k = 1,...,K$, threshold $\tau$, (e.g. $\tau = 10^{-6}$), and an integer $R'$ (e.g. $R' = 5$)
● Output: $R$ estimated unmixing matrices $B_r$ with aligned permutations
● Implementation:
  $B_r \leftarrow I_N$, $\gamma_{old} \leftarrow 0$, $\zeta \leftarrow \tau + 1$.
  if $R < R'$ do
    Exclude intra-set statistical target matrices $C_{r,r,k}$ (Remark 4)
  end
  while $\zeta \geq \tau$ do
    The U-stage: $U_r \leftarrow I_N$
    for all $1 < j \leq N$ do
        - Obtain optimal elementary upper-triangular matrices $T'_{r,(i,j)}$ for $1 \leq r \leq R$, $1 \leq i < j$ by (17), in parallel manner (Remark 3);
        - Update target matrices according to (10), and update matrices: $U_r \leftarrow T'_{r,(i,j)} U_r$
    end for
    The L-stage: $L_r \leftarrow I_N$
    for all $1 \leq j < N$ do
        - Obtain optimal elementary lower-triangular matrices $T_{r,(i,j)}$ for $1 \leq r \leq R$, $j < i \leq N$ by (17), in parallel manner (Remark 3);
        - Update target matrices according to (10) and update matrices: $L_r \leftarrow T_{r,(i,j)} L_r$
    end for
    - $B_r \leftarrow L_r U_r B_r$, $\gamma_{new} \leftarrow \max_r \| \prod_{i,j} T_{r,(i,j)} \prod_{i,j} T'_{r,(i,j)} - I_N \|_F$ (Remark 5)
    - $\zeta \leftarrow |\gamma_{new} - \gamma_{old}|$, $\gamma_{old} \leftarrow \gamma_{new}$
    - Normalize $B_r$ and $C_{r_1,r_2,k}$ according to Remark 6
end while
```

sufficiently close to the identity matrix. That is to say, we shall stop the iterations if the following inequality is met:

$$\max_{r} \left\| \prod_{i,j} \boldsymbol{T}_{r,(i,j)} \prod_{i,j} \boldsymbol{T'}_{r,(i,j)} - \boldsymbol{I}_N \right\|_F \leq \tau \qquad (20)$$

where $\boldsymbol{T}_{r,(i,j)}$ and $\boldsymbol{T'}_{r,(i,j)}$ denote the elementary rotation matrices in the L and U stages, respectively, and τ is a preset threshold (e.g., we use $\tau = 10^{-6}$ in experiments).

Remark 6 (Normalization): It is important to note that the convergence of the proposed algorithm does not necessarily imply joint diagonalization for all the asymmetric NJD datasets, as the criterion (6) is not scale invariant, and this may result in inaccurate estimates of $\alpha_{r,(i,j)}$ especially when N and K are large [11]. In practice, an efficient way to alleviate this is normalization [10]. It is simply achieved by multiplying $\tilde{\boldsymbol{B}}_r$ from the right by a diagonal matrix $\boldsymbol{D}_r$ such that each row of $\tilde{\boldsymbol{B}}_r$ is of unit norm, and multiplying $\boldsymbol{C}_{r_1,r_2,k}$ by $\boldsymbol{D}_{r_1}^{-1}$ and $\boldsymbol{D}_{r_2}^{-H}$ on both sides. In addition, we note that the computation cost of normalization for each sweep is $\mathcal{O}(KR^2N^2)$ which is negligible compared to the overall complexity. Moreover, we have observed in our experiments that the proposed algorithm still converges without normalization. However, there is no theoretical proof for such observations, and we still use it as a proper precaution.

Based on the description of GNJD algorithm and remarks in Subsections III.A and III.B, we summarize the proposed GNJD algorithm in Table I.

IV. EXPERIMENT RESULTS

In this section, we illustrate the performances of the proposed GNJD algorithm with 5 progressively more complex experiments (the list of compared algorithms may vary for different experiments and is specified at the beginning of each experiment). More exactly, we illustrate in Experiment 1 behaviors of compared algorithms with exactly diagonalizable matrices, with emphasis on the converging patterns. In Experiment 2, approximately jointly diagonalizable asymmetric target matrices are used in order to examine the performances in turbulences. In Experiment 3, we test the performance of compared algorithms in the context of 2nd-order J-BSS. In Experiment 4 and 5, results with real-world datasets are presented, wherein applications with electrocardiogram (ECG) mixtures and frequency domain speech mixtures are taken into consideration.

All the experiments are done under following configurations; CPU: Intel Core i7-4930MX 3.0 GHz; Memory: 32 GB; System: 64 bit Windows 7; Matlab R2013b.

Experiment 1. Performances With Exactly Diagonalizable Matrices: In this experiment, we demonstrate and compare the convergence behaviors of generalized JD algorithms including GNJD, NOJoB [26], JNJD [27] and GOJD [24]. We generate $K(R+1)R/2$ target matrices $\boldsymbol{C}_{r_1,r_2,k} \in \mathbb{C}^{N \times N}$, $1 \leq r_1 \leq r_2 \leq R, 1 \leq k \leq K$, according to (4) where both the real and imaginary parts of the elements of $\boldsymbol{A}_{r_1}, \boldsymbol{A}_{r_2} \in \mathbb{C}^{N \times N}$ and the diagonal elements of $\boldsymbol{D}_{r_1,r_2,k} \in \mathbb{C}^{N \times N}$ are drawn from normal distributions with zero mean and unit variance, K, R, and N denote the number of target matrices in each (asymmetric) NJD set, number of mixing matrices to be estimated, and matrix dimensionalities, respectively. The overall off-norm (ORON) at the ith sweep is calculated to evaluate the converging procedure which is defined as follows:

$$\mathrm{ORON}(i) = \frac{\sum_{r_1,r_2,k} \left\| \mathrm{off}\left(\boldsymbol{B}_{r_1}^{(i)} \cdot \boldsymbol{C}_{r_1,r_2,k} \cdot \boldsymbol{B}_{r_2}^{(i)H} \right) \right\|_F^2}{\sum_{r_1,r_2,k} \left\| \mathrm{diag}(\boldsymbol{B}_{r_1}^{(i)} \cdot \boldsymbol{C}_{r_1,r_2,k} \cdot \boldsymbol{B}_{r_2}^{(i)H}) \right\|_F^2} \qquad (21)$$

where $\boldsymbol{B}_r^{(i)}$ denotes update of the rth unmixing matrix in the ith sweep, operations '$\mathrm{off}(\cdot)$' and '$\mathrm{diag}(\cdot)$' set the diagonal and off-diagonal elements of their entries to zero, respectively.

We perform GNJD and NOJoB upon the above generated target matrices. For JNJD, the target matrices are selected from those for GNJD by requiring $r_2 = r_1 + 1$. In addition, the target matrices for GOJD are $\boldsymbol{P}_{r_1} \boldsymbol{C}_{r_1,r_2,k} \boldsymbol{P}_{r_2}^H$ for all $1 \leq r_1 \leq r_2 \leq R$, $1 \leq k \leq K$, where $\boldsymbol{P}_r$ is the pre-whitening matrix obtained from singular value decomposition (SVD) of $\boldsymbol{A}_r$. We draw the ORON curves of the compared algorithms versus the number of sweeps from 10 independent runs, under the following settings: (a) $K = 20, N = 5, R = 3$; (b) $K = 20, N = 5, R = 10$; (c) $K = 20, N = 5, R = 15$; (d) $K = 20, N = 5, R = 20$. The results are plotted in Fig. 1. We note here that in all the 4 settings, both GNJD and GOJD converge nicely within 15 sweeps, with superlinear converging pattern particularly when approaching the final solution. In contrary, we note that non-optimal converging patterns exist for NOJoB in settings (b), (c), and (d), which are at times observed to fail to converge into global minimum. This suggests that using NOJoB for large number of datasets is likely to have problems of permutation misalignment. In addition, JNJD almost completely fail to converge into global minimum in settings (b), (c), and (d). The above observations suggest that GOJD and the proposed GNJD algorithms are the most reliable ones among the competitors in achieving both estimation of loading matrices and permutation alignment, when handling small or large number of datasets. On the other hand, NOJoB provides quite reliable performance when the number of datasets is small, yet lacks some efficiency for large number of datasets as is indicated in the non-optimal converging patterns. JNJD is only able to handle small number of datasets.

It is important to note that in this experiment perfect pre-whitening is done for GOJD, noting that the matrices $\boldsymbol{P}_r$ are obtained with SVD of the true loading matrices $\boldsymbol{A}_r$, $r = 1, 2, \ldots, R$. However, in noisy cases where uncorrectable errors for subsequent GOJD stage are likely to be introduced in pre-whitening [23], the performance of GOJD will deteriorate, as will be shown in following experiments.

Experiment 2. Performances With Approximately Jointly Diagonalizable Matrices: In this experiment, we examine and compare the performances of generalized JD algorithms (GNJD, NOJoB, GOJD, JNJD) with approximately jointly diagonalizable target matrices generated as follows:

$$\boldsymbol{C}'_{r_1,r_2,k} = \sigma_s \frac{\boldsymbol{C}_{r_1,r_2,k}}{\|\boldsymbol{C}_{r_1,r_2,k}\|_F} + \sigma_n \frac{\boldsymbol{N}_{r_1,r_2,k}}{\|\boldsymbol{N}_{r_1,r_2,k}\|_F} \tag{22}$$

where $\boldsymbol{C}_{r_1,r_2,k}$ is constructed in the same way as Experiment 1, $\boldsymbol{N}_{r_1,r_2,k}$ is the noise term with both the real and imaginary parts drawn from normal distributions with zero mean and unit variance, and σ_s, σ_n denote the levels of signal and noise, respectively. In addition, we define signal-to-noise ratio (SNR) in this case as:

$$\text{SNR} = 10 \log_{10}(\sigma_s/\sigma_n) \tag{23}$$

We perform GNJD and NOJoB upon $\boldsymbol{C}'_{r_1,r_2,k}$, $r_1 = 1, 2, \ldots, R$, $r_2 = r_1, \ldots, R$, $k = 1, 2, \ldots, K$, and JNJD upon the subset of $\boldsymbol{C}'_{r_1,r_2,k}$ with $r_2 = r_1 + 1$. In addition, the true loading matrices $\boldsymbol{A}_r$ are assumed known for GOJD to facilitate pre-whitening. The target matrices for GOJD are $\boldsymbol{P}_{r_1}\boldsymbol{C}'_{r_1,r_2,k}\boldsymbol{P}^H_{r_2}$ with pre-whitening matrices $\boldsymbol{P}_r$ obtained from SVD of $\boldsymbol{A}_r$, $r = 1, 2, \ldots, R$.

We evaluate the performances of all compared algorithms by the joint inter-symbol-interference (J-ISI) [24] defined as:

$$\begin{aligned}\mathrm{J-ISI}(\boldsymbol{G}) \triangleq \frac{1}{2N(N-1)} &\left[\sum_{i=1}^{N}\left(\sum_{j=1}^{N}\frac{g_{ij}}{\max_k g_{ik}} - 1\right)\right. \\ &\left. + \sum_{j=1}^{N}\left(\sum_{i=1}^{N}\frac{g_{ij}}{\max_k g_{kj}} - 1\right)\right]\end{aligned} \tag{24}$$

where g_{ij} denotes the (i, j)th element of $\boldsymbol{G} \triangleq \sum_{r=1}^{R} |\boldsymbol{W}_r \boldsymbol{A}_r|$, $|\cdot|$ calculates the absolute value of each element of its entry, $\boldsymbol{W}_r$ denotes the rth normalized estimated unmixing matrix, and $\boldsymbol{A}_r$ is the rth normalized true mixing matrix. We note here that J-ISI takes into account both the accuracy and the permutation of the rows of the estimates of unloading matrices, and a small value of it indicates an accurate estimate of each individual unmixing matrix, as well as nicely aligned permutations for all the unmixing matrices.

We fix σ_n to 0.01, let SNR vary from 0–20 dB, and plot the J-ISI curves obtained from 100 independent runs in Fig. 2 under the following two settings: (a) $K = 20, N = 5, R = 5$; (b) $K = 20, N = 5, R = 20$. It is shown that GNJD provides the

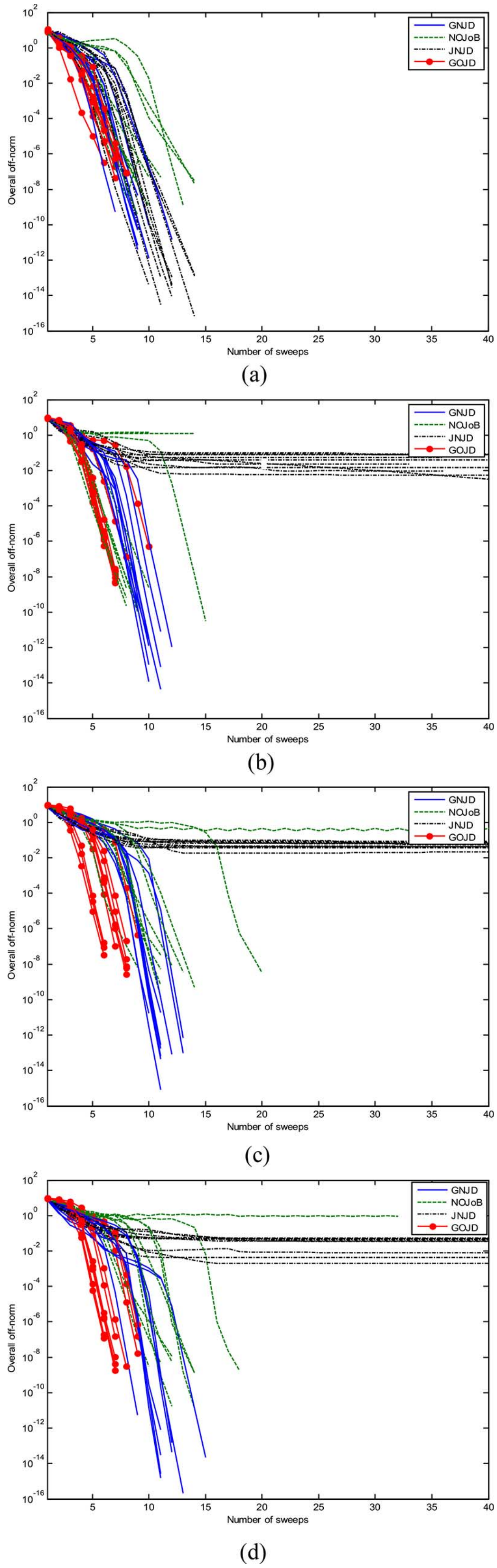

(a)

(b)

(c)

(d)

Fig. 1. Overall off-norm (ORON) of GNJD, NOJoB, JNJD, and GOJD versus the number of sweeps. (a) $N = 5, R = 3, K = 20$, (b) $N = 5, R = 10, K = 20$, (c) $N = 5, R = 15, K = 20$, (d) $N = 5, R = 20, K = 20$.

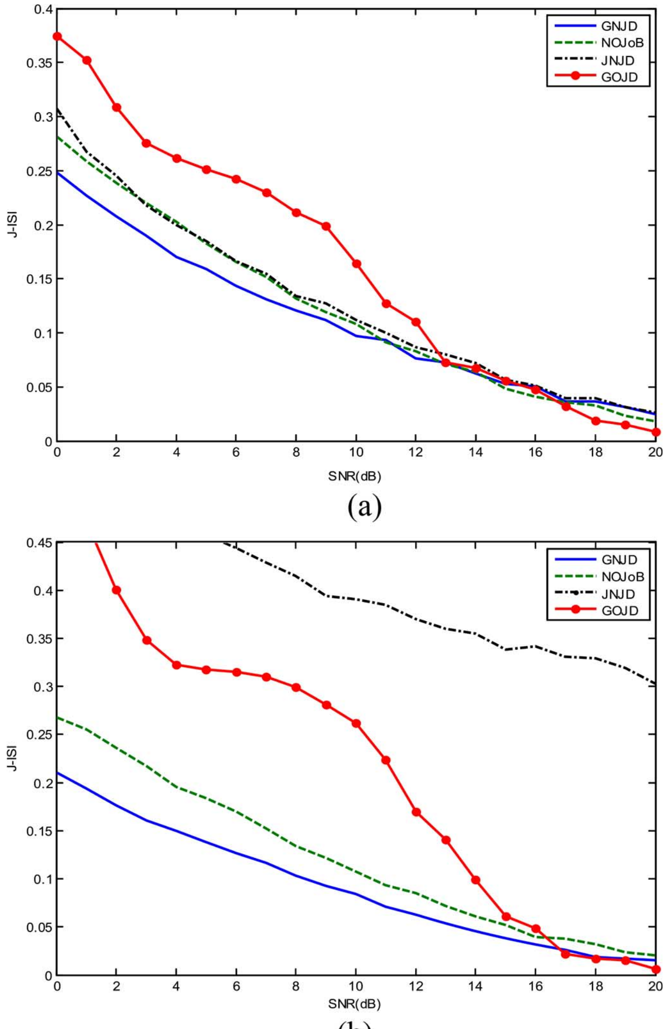

(a)

(b)

Fig. 2. J-ISI of GNJD, NOJoB, JNJD, GOJD in additive turbulences. (a) $N = 5, R = 5, K = 20$, (b) $N = 5, R = 20, K = 20$.

best results when SNR is lower than 16 dB, followed by NOJoB and then by GOJD in both cases. This observation clearly indicates the pros and cons of non-orthogonal and orthogonal GJD that the former is likely to outperform the latter in the presence of additive turbulences, and this coincides nicely with the comparison of the non-orthogonal and the orthogonal in the JD context [32]. Moreover, it is interesting to note that JNJD provides competitive performance when $R = 5$, which again suggests its applicability for small number of datasets.

Experiment 3. 2nd-Order J-BSS of Synthetic Multi-Set Data: In this experiment, we compare the proposed GNJD algorithm with NOJoB, GOJD, and MCCA in 2nd-order J-BSS of synthetic multi-set data (JNJD is excluded due to its poor performance in the following settings). The non-stationary sources are generated as:

$$\boldsymbol{s}_n(t) = \boldsymbol{\Pi}\boldsymbol{s'}_n(t) \tag{25}$$

where $\boldsymbol{s}_n(t) \triangleq [s_n^{(1)}(t), s_n^{(2)}(t), \ldots, s_n^{(R)}(t)]^T \in \mathrm{C}^R$, $s_n^{(r)}(t)$ denotes the nth source at time instance t in the rth dataset, and $\boldsymbol{\Pi} \in \mathrm{C}^{R\times R}$ is a full rank matrix used to introduce inter-set correlations. Both the real and imaginary parts of each element of $\boldsymbol{\Pi}$ are drawn from normal distribution of zero mean and unit variance. $\boldsymbol{s'}_n(t) \triangleq [{s'}_n^{(1)}(t), \ldots, {s'}_n^{(R)}(t)]^T$ are complex BPSK that are amplitude modulated across time slots:

$${s'}_n^{(r)}(t) = \sum_{m=1}^{M} \eta_m {s'}_{n,m}^{(r)}(t) \tag{26}$$

where η_m's are randomly drawn from uniform distribution over [0, 1] and ${s'}_{n,m}^{(r)}(t)$ is defined as:

$${s'}_{n,m}^{(r)}(t) = \begin{cases} b^{(m)}(t-m(1-\alpha)L), & m(1-\alpha)L < t \leq m(1-\alpha)L+L \\ 0, & \text{else} \end{cases} \tag{27}$$

where $b^{(m)}(t)$ is a BPSK signal at time t with value selected from symbols $[1+\vec{\mathrm{i}}, 1-\vec{\mathrm{i}}]$ with equal probability, L is the number of samples of $b^{(m)}(t)$, and α denotes the overlapping rate of parts in $b^{(m-1)}(t)$ and $b^{(m)}(t)$ that contribute to the same time duration in ${s'}_n^{(r)}(t)$. The mixtures are constructed as:

$$\boldsymbol{x}_r(t) = \sigma_s \frac{\boldsymbol{A}_r\boldsymbol{s}^{(r)}(t)}{\|\boldsymbol{A}_r\boldsymbol{s}^{(r)}(t)\|_F} + \sigma_n \frac{\boldsymbol{n}^{(r)}(t)}{\|\boldsymbol{n}^{(r)}(t)\|_F}, \quad r = 1, 2, \ldots, R \tag{28}$$

where both the real and imaginary parts of mixing matrices $\boldsymbol{A}_r$'s are taken randomly from normal distribution with zero mean and unit variance, and $\boldsymbol{n}^{(r)}(t)$ is the noise term in the rth dataset. The spatial correlations for noise terms associated with distinct datasets are introduced similarly to (25). σ_s and σ_n denote the signal and noise levels respectively. We note here that ${s'}_n^{(r)}(t)$ (see Fig. 3 as an example) are short-time stationary, and thus target matrices $\boldsymbol{C}_{r_1,r_2,k}$ are constructed according to (5). In practice, we calculate the sampled version of $\boldsymbol{C}_{r_1,r_2,k}$ as:

$$\tilde{\boldsymbol{C}}_{r_1,r_2,k} = \frac{1}{L'} \sum_{t=1}^{L'} \boldsymbol{x}_{r_1,k}(t)\boldsymbol{x}_{r_2,k}^H(t) \tag{29}$$

where $\boldsymbol{x}_{r,k}(t)$ denotes the kth block segmented from $\boldsymbol{x}_r(t)$ along the time dimension, with block length L', and overlapping rate $\alpha' \in [0, 1]$. SNR in this scenario is defined with σ_s and σ_n via (23).

The target matrices for GOJD are obtained with pre-whitened datasets. The pre-whitening matrices are obtained via SVD of the sampled $\boldsymbol{x}_r(t)$. The target matrices for MCCA are cross-covariance matrices (without taking into account the temporal non-stationarity) across every pair of pre-whitened datasets.

We fix the number of temporal samples $T = 2000$, $L = 200$, $L' = 100$, and $\alpha = \alpha' = 0.5$, and let SNR vary from -2 dB–10 dB. The J-ISI curves versus SNR are plotted in Fig. 4 with contributions from 100 independent runs under the following 2 settings: (a) $N = 5, R = 10$; (b) $N = 5, R = 20$.

From Fig. 4 we see that GNJD yields best performance in low SNR levels (-2–5 dB), followed by NOJoB, and GOJD in both scenarios. When SNR exceeds 5 dB, the proposed GNJD algorithm slightly underperforms NOJoB and GOJD, but is still able to provide quite precise estimates (J-ISI is below 0.05). In addition, the merit of GNJD in low SNR is seen clearer when

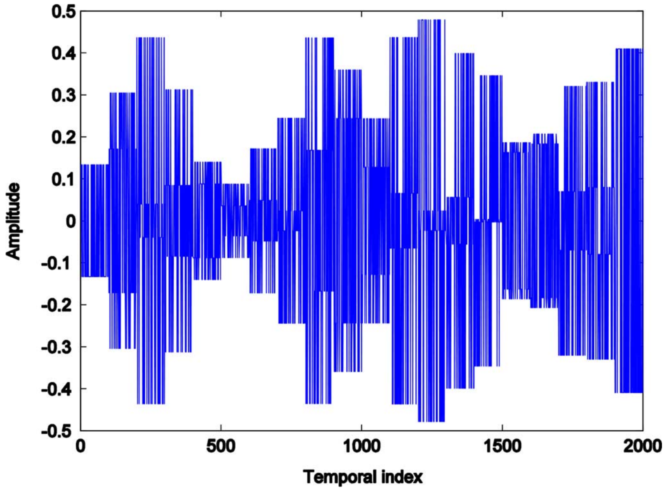

Fig. 3. The real part of an amplitude modulated BPSK signal with $L = 200$, and $\alpha = 0.5$.

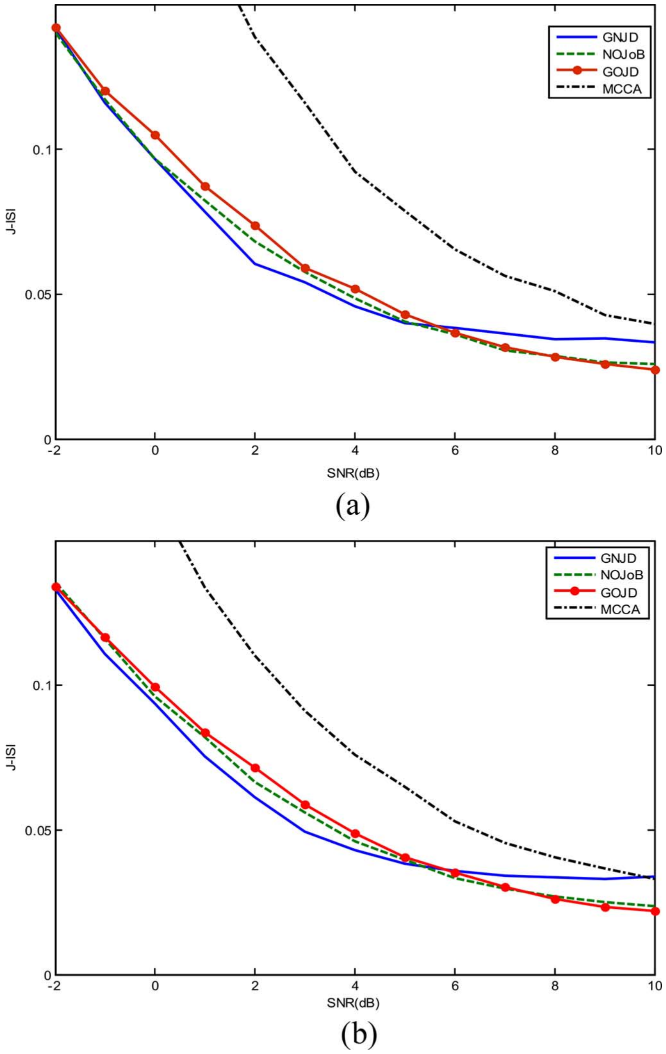

(a)

(b)

Fig. 4. J-ISI of GNJD, NOJoB, GOJD, and MCCA in 2nd-order J-BSS. (a) $N = 5, R = 10$, (b) $N = 5, R = 20$.

$R = 20$, suggesting that the proposed GNJD algorithm is more advantageous for handling larger number of datasets.

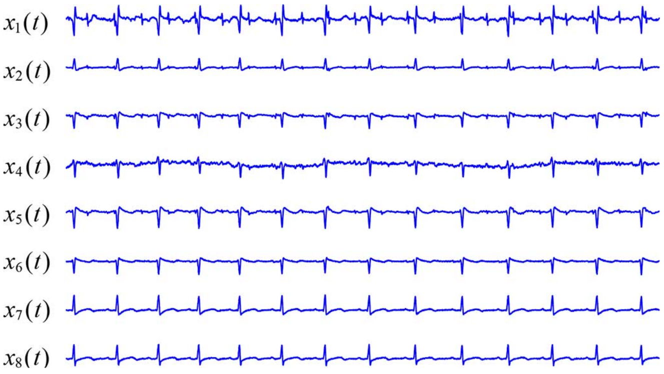

Fig. 5. The 8-channel ECG data from a pregnant woman.

We note in this experiment (as well as Experiment 2) that GNJD exhibits slightly lower performance than GOJD and NOJoB for high SNR's. That is because the latter two algorithms impose some constraints in the optimization (e.g., the orthogonality constraint for GOJD, the unit-norm constraint for rows of demixing matrix in NOJoB), and these constraints bring some merits over the unconstrained GNJD algorithm when SNR is high (such that prewhitening is precise for GOJD and non-optimal convergence is rarely encountered for NOJoB). In the presence of low SNR, however, that GOJD suffers from imprecise prewhitening and NOJoB encounters non-optimal convergence, GNJD is shown to yield best performance. In fact, noise is always present and can sometimes be quite high in real-world problems, and that makes GNJD particularly interesting in solving practical noisy problems.

Experiment 4. Fetal Electrocardiogram (ECG) Separation: In this experiment, we consider and compare 2nd-order J-BSS with GNJD, JNJD, GOJD, NOJoB, and MCCA in the context of fetal ECG separation with real-world 8-channel ECG data as is shown in Fig. 5, collected from a pregnant woman and made available in [33]. The sampling rate is 250 Hz and 2500 samples (10 s) are recorded.

We note that the 2nd-order J-BSS with GOJD has already been applied to the same dataset and more details about the motivation of using J-BSS in such problems could be found in [24]. Here, we emphasize on the comparison of J-BSS algorithms in this application. The multi-set data is constructed following a similar procedure to [24] as:

$$\boldsymbol{x}_r(t) = [x_r(t), x_{r+1}(t), x_{r+2}(t), x_{r+3}(t)]^T, \quad r = 1, 2, 3, 4, 5 \tag{30}$$

The target matrices for GNJD and NOJoB are non-stationary covariance matrices, obtained similarly to (29) in Experiment 3 with block length $L' = 200$, and overlapping rate $\alpha' = 0.5$. The target matrices for JNJD and GOJD are constructed from those of GNJD via a similar procedure to that in Experiment 3. The target matrices for MCCA are cross-covariance matrices across every pair of pre-whitened datasets. The separation results are plotted in Figs. 6–10 where those labelled $\boldsymbol{y}_r(t)$ denote the rth set of estimated sources, $r = 1, \ldots, 5$.

From those figures we see that the strong and slow mother ECG could be nicely extracted by all the 5 compared algorithms, if we note the last two columns of the displayed results

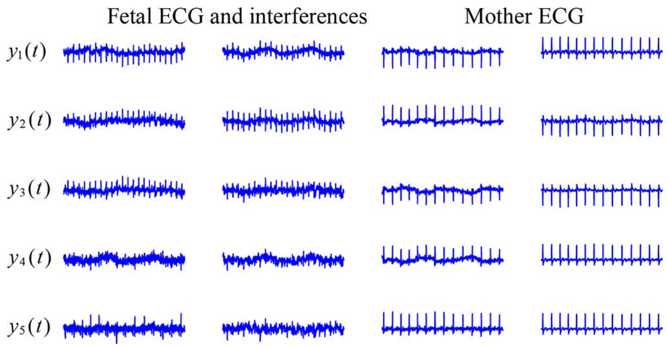

Fig. 6. Results from J-BSS with GNJD.

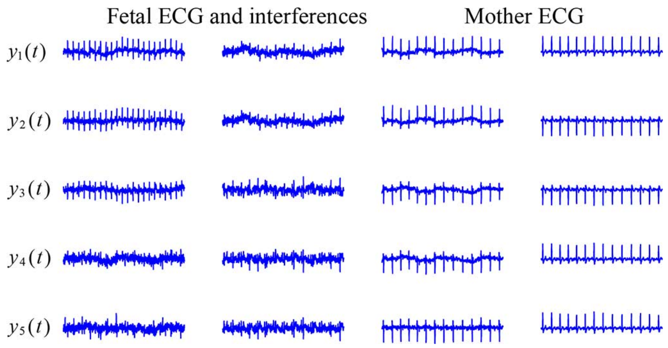

Fig. 7. Results from J-BSS with GOJD.

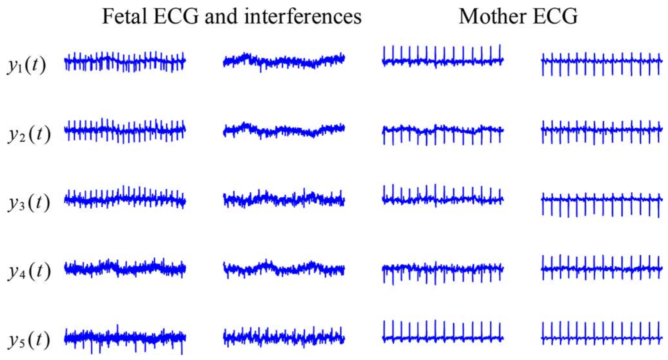

Fig. 8. Results from J-BSS with JNJD.

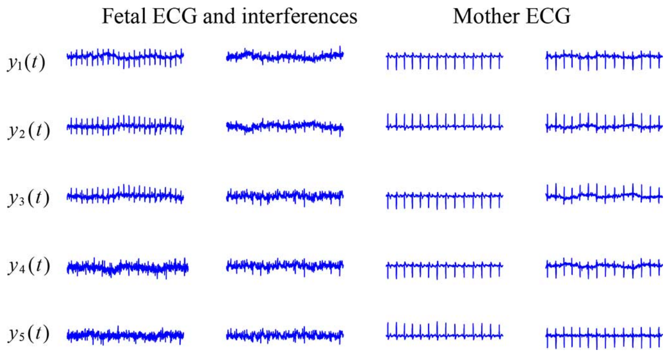

Fig. 9. Results from J-BSS with NOJoB.

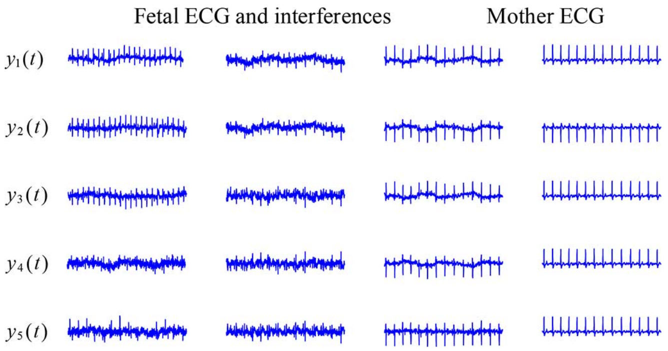

Fig. 10. Results from J-BSS with MCCA.

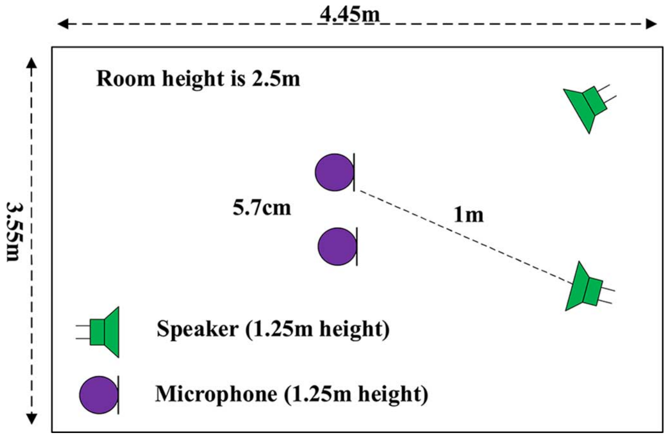

Fig. 11. Illustration of the simulated room settings.

in Figs. 6–10. In addition, the fetal ECG could be successfully restored in some components of the estimated results as well, if we look into the 1st components in $\boldsymbol{y}_1(t)$, $\boldsymbol{y}_2(t)$, and $\boldsymbol{y}_3(t)$ for all the compared algorithms. However, differences could be observed in other estimated results. In particular, we note that GNJD extracts more components related to fetal ECG than others if we compare the 2nd column of the displayed results, where GOJD, JNJD, NOJoB and MCCA only generate interferences while GNJD extracts fetal ECG components in $\boldsymbol{y}_1(t)$ and $\boldsymbol{y}_2(t)$. Generally, fetal ECG's are with particular interests in this application.

Experiment 5. Speech Separation in Frequency Domain: In this experiment, we consider and compare the applications of 2nd-order J-BSS with GNJD, JNJD, GOJD, NOJoB and MCCA to real-world speech separation in the frequency domain. We also include in the comparison some JD algorithms such as Cardoso's Jacobi-like OJD algorithm [1], Tichavsky and Yeredor's uniformly weighted exhaustive diagonalization by Gaussian iteration (UWEDGE) [6], complex-valued joint diagonalization via givens and shear rotations (C-JDi) [13] proposed by Mesloub, Abed-Meraim, and Belouchrani, and LU decomposition based complex-valued JD (LUCJD) [12]. We consider the scenario that two microphones receive two speeches. The real-world mixtures are obtained from SISEC2010 website [34] (scenarios Room 4 and Room 5). The room is a chamber with cushion walls of size 4.45 m × 3.55 m × 2.5 m, microphones are placed around the center of the room with height 1.25 m with interspacing of 5.7 cm, the sources are placed at height 1.25 m, with distance of 1 m from microphones in Room 4 setting, and 1.8 m from microphones in Room 5 setting. The detailed description of the scenarios could be found in [34], and an illustration of Room 4 is given in Fig. 11.

Frequency domain speech mixtures are obtained with short time Fourier transform (STFT). The STFT frames are of length F ($F = 2048$ or 4096 in particular) for the competitors, half-overlapped with neighboring ones and windowed with sine function. The signals for the first $N_{\mathrm{bin}} = F/2 + 1$ frequency bins are selected for the compared algorithms, as the rest of the frequency bins are redundant due to the symmetry of Fourier transform. The Matlab code for the above procedure could be found in E. Vincent's website [35].

In addition, we construct $\lfloor N_{\mathrm{bin}}/R \rfloor$ groups each containing R adjacent frequency bins, and perform 2nd-order J-BSS described in Subsection II.B with GNJD, GOJD, JNJD, NOJoB, and MCCA for each group. For JD algorithms including OJD, UWEDGE, C-JDi, and LUCJD, 2nd-order BSS is performed for each frequency bin wherein the target matrices are obtained as non-stationary covariance matrices [3]. Moreover, pre-whitening is done at each frequency bin for OJD, MCCA, and GOJD.

After the above 2nd-order J-BSS (BSS) stage for each frequency bin, we calculate cross-covariance's of amplitudes of separated signal components of adjacent frequency bins, and admit those with larger cross-covariance's as coming from the same source. This amplitude-covariance based permutation alignment scheme is then performed sequentially to cover all the frequency bins to tackle the permutation ambiguity problem. In addition, the scaling ambiguity problem is solved via minimal distortion principle [36]. It is important to note that there actually exist more advanced permutation alignment schemes in the open literature [37]. However, we emphasize herein the separation performance for each frequency bin, and thus only use the basic one. Finally, inverse STFT is done to transform the separation results back to time domain.

We obtain the source speeches from Sawada's website [38]. The performance is evaluated with signal-to-interference ratio (SIR) and signal-to-distortion ratio (SDR). Detailed definitions and Matlab codes for these metrics could be found in [35].

All the compared algorithms are performed with STFT length $F = 2048$ and $F = 4096$. In addition, J-BSS algorithms (GNJD, NOJoB, GOJD, JNJD, MCCA) are performed with $R = 3$ and $R = 4$. Over all the above parameter options, the best result (with largest average SIR value) for each individual algorithm is selected and illustrated in Tables II and III for Room 4 and 5, respectively.

We highlight the largest value along each column with bold font. From these tables we firstly observe that GNJD generates the best average results over the 2 sources in both scenarios, with regards to both SIR and SDR values. Moreover, for SIR values of each specific source, GNJD provides the best results for both sources in setting Room 4, and best SIR value for source 2 in setting Room 5. In addition, we note that GNJD is able to yield nice SIR's for both sources, in contrary to some other algorithms that only yield nice estimate for one source yet poor one for the other (e.g., NOJoB and GOJD in setting Room 5). Noting that SIR generally evaluates the separatability of the compared algorithms, the superiority of GNJD over all other competitors with regards to SIR clearly indicates its advantages in this aspect. Furthermore, we note that GNJD is able to provide quite competent SDR values (always ranked among top 3 for each specific source in both settings, and ranked 1st for the average value), indicating that GNJD could provide nice quality of the resulting speech estimates in addition to nice separatability.

TABLE II
SIR AND SDR VALUES OF ALL COMPARED ALGORITHMS FOR SEPARATING REAL-WORLD SPEECH MIXTURES UNDER SCENARIO ROOM 4

Method	Results for source 1		Results for source 2		Average results	
	SIR$_1$	SDR$_1$	SIR$_2$	SDR$_2$	SIR$_{\mathrm{ave}}$	SDR$_{\mathrm{ave}}$
GNJD	**18.99**	12.25	**19.39**	11.76	**19.19**	**12.00**
NOJoB	8.60	5.13	15.07	10.07	11.83	7.60
GOJD	8.92	5.67	16.44	10.24	12.69	7.96
JNJD	12.94	8.18	16.97	10.48	14.95	9.33
MCCA	11.31	9.21	6.56	5.81	8.94	7.51
OJD	12.24	7.77	18.13	11.41	15.18	9.59
UWEDGE	18.77	**13.11**	11.60	7.76	15.18	10.43
C-JDi	10.29	7.36	18.29	**11.99**	14.29	9.68
LUCJD	18.18	12.78	11.52	7.80	14.85	10.29

TABLE III
SIR AND SDR VALUES OF ALL COMPARED ALGORITHMS FOR SEPARATING REAL-WORLD SPEECH MIXTURES UNDER SCENARIO ROOM 5

Method	Results for source 1		Results for source 2		Average results	
	SIR$_1$	SDR$_1$	SIR$_2$	SDR$_2$	SIR$_{\mathrm{ave}}$	SDR$_{\mathrm{ave}}$
GNJD	14.40	5.78	**21.27**	**11.61**	**17.84**	**8.70**
NOJoB	4.67	1.47	18.96	10.70	11.82	6.08
GOJD	14.86	8.18	5.29	1.95	10.11	5.27
JNJD	9.91	5.21	17.33	9.83	13.62	7.52
MCCA	7.15	3.97	1.67	-0.59	4.41	1.69
OJD	9.36	5.03	18.41	10.30	13.89	7.67
UWEDGE	**17.20**	**10.25**	9.29	3.92	13.24	7.09
C-JDi	8.46	4.09	17.27	9.92	12.87	7.00
LUCJD	9.40	4.55	17.48	9.74	13.44	7.14

The results clearly demonstrate the superiority of GNJD over other (generalized) JD variants in frequency domain based speech separation, thanks to its strong and robust performance for exploiting inter-set covariances of multi-set data in highly noisy environments.

V. CONCLUSION

In this study, we considered the generalized non-orthogonal joint diagonalization (GNJD) of multiple asymmetric NJD datasets of which every pair share one common loading matrix. We proposed an algorithm for such problem based on LU decompositions and successive rotations. We have shown that the GNJD formulization could be obtained from the multi-set data model by using 2nd-order statistics, and thus the proposed algorithm could be used in multi-set data analysis applications such as joint blind source separation (J-BSS) and multi-modal/multi-subject data fusion. In addition, we have provided some theoretical analysis including complexity and convergence, as well as some implementation remarks.

Experiments are conducted to compare the proposed GNJD algorithm with existing ones of similar type, namely non-orthogonal joint blind source separation (NOJoB), generalized orthogonal joint diagonalization (GOJD), joint NJD (JNJD), and multiple canonical correlation analysis (MCCA), with artificial target matrices in both exactly and approximately jointly diagonalizable cases (Experiments 1 and 2), 2nd-order J-BSS applications over synthetic datasets (Experiment 3), and real-world J-BSS applications such as fetal ECG extraction (Experiment 4), and frequency domain speech separation (Experiment 5). The results generally show that GNJD is able to provide better performance when compared with NOJoB, GOJD, JNJD, and MCCA.

The sensitivities of GNJD and other generalized JD methods to difficult conditions are not studied in this paper and will be one of our future focuses.

Acknowledgment

The authors would like to express sincere gratitude to Dr. M. Congedo for providing us with source programs of NOJoB algorithm in [26]. We would also like to thank Prof. K. Abed-Meraim, and his student A. Mesloub for providing us with source programs of C-JDi algorithm in [13]. The authors are also grateful for the anonymous reviewers for their helpful comments and suggestions.

References

[1] J.-F. Cardoso and A. Souloumiac, “Blind beamforming for non-Gaussian signals,” *Proc. Inst. Electr. Eng.—F, Radar, Signal Process.*, vol. 140, no. 6, pp. 362–370, Dec. 1993.

[2] A. Belouchrani, K. Abed-Meraim, and J.-F. Cardoso, “A blind source separation technique using second-order statistics,” *IEEE Trans. Signal Process.*, vol. 45, no. 2, pp. 434–444, Feb. 1997.

[3] D.-T. Pham, C. Servière, and H. Boumaraf, “Blind separation of convolutive audio mixtures using nonstationarity,” presented at the ICA, Nara, Japan, Apr. 1–4, 2003.

[4] A. Yeredor, “Blind separation of Gaussian sources with general covariance structures: Bounds and optimal estimation,” *IEEE Trans. Signal Process.*, vol. 58, no. 10, pp. 5057–5068, Oct. 2010.

[5] A. Yeredor, “Non-orthogonal joint diagonalization in the least-squares sense with application in blind source separation,” *IEEE Trans. Signal Process.*, vol. 50, no. 7, pp. 1545–1553, Jul. 2002.

[6] P. Tichavský and A. Yeredor, “Fast approximate joint diagonalization incorporating weight matrices,” *IEEE Trans. Signal Process.*, vol. 57, no. 3, pp. 878–891, Mar. 2009.

[7] X.-L. Li and X.-D. Zhang, “Nonorthogonal joint diagonalization free of degenerate solution,” *IEEE Trans. Signal Process.*, vol. 55, no. 5, pp. 1803–1814, May 2007.

[8] A.-J. van der Veen, “Joint diagonalization via subspace fitting techniques,” presented at the ICASSP, Salt Lake City, UT, USA, Mar. 07–11, 2001.

[9] A. Ziehe, P. Laskov, G. Nolte, and K. R. Muller, “A fast algorithm for joint diagonalization with non-orthogonal transformations and its application to blind source separation,” *J. Mach. Learn. Res.*, vol. 5, pp. 777–800, Jul. 2004.

[10] A. Souloumiac, “Nonorthogonal joint diagonalization by combining Givens and Hyperbolic rotations,” *IEEE Trans. Signal Process.*, vol. 57, no. 6, pp. 2222–2231, Jun. 2009.

[11] B. Afsari, “Simple LU and QR based non-orthogonal matrix joint diagonalization,” presented at the ICA, Charleston, SC, USA, Mar. 5–8, 2006.

[12] K. Wang, X.-F. Gong, and Q.-H. Lin, “Complex non-orthogonal joint diagonalization based on LU and LQ decompositions,” presented at the LVA/ICA’2012, Tel Aviv, Israel, Mar. 12–15, 2012.

[13] A. Mesloub, K. Abed-Meraim, and A. Belouchrani, “A new algorithm for complex non-orthogonal joint diagonalization based on shear and givens rotations,” *IEEE Trans. Signal Process.*, vol. 62, no. 8, pp. 1913–1925, Apr. 2014.

[14] D.-T. Pham, “Joint approximate diagonalization of positive definite matrices,” *SIAM J. Matrix Anal. Appl.*, vol. 23, no. 4, pp. 1136–1152, Apr. 2001.

[15] J.-H. Lee, T.-W. Lee, F. Jolesz, and S.-S. Yoo, “Independent vector analysis (IVA): Multivariate approach for fMRI group study,” *NeuroImage*, vol. 40, no. 1, pp. 86–109, Mar. 1, 2008.

[16] T. Kim, H. T. Attias, S.-Y. Lee, and T.-W. Lee, “Blind source separation exploiting higher-order frequency dependencies,” *IEEE Trans. Audio, Speech, Lang. Process.*, vol. 15, no. 1, pp. 70–79, Jan. 2007.

[17] M. Anderson, T. Adali, and X.-L. Li, “Joint blind source separation with multivariate Gaussian model: Algorithms and performance analysis,” *IEEE Trans. Signal Process.*, vol. 60, no. 4, pp. 1672–1683, Apr. 2012.

[18] H. Hotelling, “Relations between two sets of variates,” *Biometrika*, vol. 28, pp. 321–377, 1936.

[19] J. R. Kettenring, “Canonical analysis of several sets of variables,” *Biometrika*, vol. 58, no. 3, pp. 433–451, 1971.

[20] Y.-O. Li, T. Adali, W. Wang, and V. Calhoun, “Joint blind source separation by multiset canonical correlation analysis,” *IEEE Trans. Signal Process.*, vol. 57, no. 10, pp. 3918–3929, Oct. 2009.

[21] N. M. Correa, T. Eichele, T. Adali, Y.-O. Li, and V. D. Calhoun, “Multi-set canonical correlation analysis for the fusion of concurrent single trial ERP and functional MRI,” *NeuroImage*, vol. 50, no. 4, pp. 1438–1445, May 2010.

[22] N. M. Correa, T. Adali, and V. D. Calhoun, “Canonical correlation analysis for data fusion and group analysis: Examining applications of medical imaging data,” *IEEE Signal Process. Mag.*, vol. 27, no. 4, pp. 39–50, Jul. 2010.

[23] J. Chatel-Goldman, M. Congedo, and R. Phlypo, “Joint BSS as a natural analysis framework for EEG-hyperscanning,” presented at the ICASSP, Vancouver, Canada, May 26–30, 2013.

[24] X.-L. Li, T. Adalí, and M. Anderson, “Joint blind source separation by generalized joint diagonalization of cumulant matrices,” *Signal Process.*, vol. 91, no. 10, pp. 2314–2322, Oct. 2011.

[25] M. Congedo, R. Phlypo, and D.-T. Pham, “Approximate joint singular value decomposition of an asymmetric rectangular matrix set,” *IEEE Trans. Signal Process.*, vol. 59, no. 1, pp. 415–424, Jan. 2011.

[26] M. Congedo, R. Phlypo, and J. Chatel-Goldman, “Orthogonal and non-orthogonal joint blind source separation in the least-squares sense,” presented at the EUSIPCO, Bucharest, Romania, Aug. 27–31, 2012.

[27] X.-F. Gong, Q.-H. Lin, and K. Wang, “Joint non-orthogonal joint diagonalization based on LU decomposition and Jacobi scheme,” presented at the CHINASIP, Beijing, China, Jul. 6–10, 2013.

[28] L. De Lathauwer and J. Castaing, “Tensor-based techniques for the blind separation of DS-CDMA signals,” *Signal Process.*, vol. 87, no. 2, pp. 322–336, Feb. 2007.

[29] X.-F. Gong, Y.-N. Hao, and Q.-H. Lin, “Joint canonical polyadic decomposition of two tensors with one shared loading matrix,” presented at the MLSP, Southampton, U.K., Sep. 22–25, 2013.

[30] X.-L. Wang, X.-F. Gong, and Q.-H. Lin, “A study on parallelization of successive rotation based joint diagonalization,” presented at the DSP, Hong Kong, China, Aug. 20–23, 2014.

[31] A. Holobar, M. Ojstersek, and D. Zazula, “A new approach to parallel joint diagonalization of symmetric matrices,” presented at the EUROCON, Ljubljana, Slovenia, Sep. 22–24, 2003.

[32] A. Souloumiac, “Joint diagonalization: Is non-orthogonal always preferable to orthogonal?,” presented at the CAMSAP, Aruba, Dutch Antilles, Dec. 13–16, 2009.

[33] D. De Moor, Ed., DAISY: Database for the Identification of Systems [Online]. Available: http://www.esat.kuleuven.ac.be/sista/daisy Available online at:

[34] Determined and over-determined speech and music mixtures [Online]. Available: http://www.irisa.fr/metiss/members/evincent/software

[35] E. Vincent, Evaluation software and audio source separation software [Online]. Available: http://www.irisa.fr/metiss/members/evincent/software

[36] K. Matsuoka and S. Nakashima, “Minimal distortion principle for blind source separation,” in *Proc. ICA*, 2001, pp. 722–727.

[37] L. Wang, H. Ding, and F. Yin, “A region-growing permutation alignment approach in frequency-domain blind source separation of speech mixtures,” *IEEE Trans. Audio, Speech, Lang. Process.*, vol. 19, no. 3, pp. 549–557, Mar. 2011.

[38] H. Sawada, BSS Sound Demonstration [Online]. Available: http://www.kecl.ntt.co.jp/icl/signal/sawada/demo/bss2to4/index.html

[39] X.-F. Gong, X.-L. Wang, and Q.-H. Lin, GNJD software package [Online]. Available: http://202.118.75.4/gong/GNJD.html

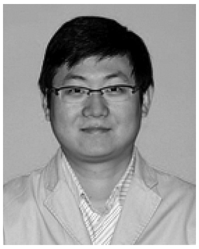

Xiao-Feng Gong (M'10) was born in the city of Yichang, Hubei province, China, in 1981. In 2003, he earned the B.S. degree (information engineering) from the Beijing Institute of Technology, China. From 2003 to 2009, he took the combined Master's and Ph.D. program of the Beijing Institute of Technology, and earned the Ph.D. degree (communication and information system) in 2009. His Ph.D. thesis concerned polarization sensitive array processing with tensors and hypercomplex numbers.

He was a lecturer from 2009 to 2012, and has been an associate professor since 2013, both with Dalian University of Technology, Dalian, China. He is currently a visiting research associate with KU Leuven Kortrijk campus, Kortrijk, Belgium. His research interests include multilinear algebra and its applications in blind source separation and array processing.

Xiu-Lin Wang was born in Dezhou city, Shandong province, China, in 1990. In 2012, he earned the B.S. degree (electronic and information engineering) from Shandong University Weihai campus, China. He is currently pursuing his M.S. degree in Dalian University of Technology, Dalian, China.

His research interests are algebraic methods for multiset signal processing.

Qiu-Hua Lin (M'10) received the B.S. degree in wireless communication, the M.S. degree in communications and electronic systems, and the Ph.D. degree in signal and information processing, all from Dalian University of Technology, Dalian, China.

She is currently a Professor at the School of Information and Communication Engineering, Dalian University of Technology, Dalian, China. Her research interests include stochastic signal processing, array signal processing, biomedical signal processing, and image processing.